Programmable *in situ* amplification for multiplexed imaging of mRNA expression

Harry M T Choi[1], Joann Y Chang[1], Le A Trinh[2], Jennifer E Padilla[1], Scott E Fraser[1,2] & Niles A Pierce[1,3]

In situ hybridization methods enable the mapping of mRNA expression within intact biological samples[1,2]. With current approaches, it is challenging to simultaneously map multiple target mRNAs within whole-mount vertebrate embryos[3–6], representing a significant limitation in attempting to study interacting regulatory elements in systems most relevant to human development and disease. Here, we report a multiplexed fluorescent *in situ* hybridization method based on orthogonal amplification with hybridization chain reactions (HCR)[7]. With this approach, RNA probes complementary to mRNA targets trigger chain reactions in which fluorophore-labeled RNA hairpins self-assemble into tethered fluorescent amplification polymers. The programmability and sequence specificity of these amplification cascades enable multiple HCR amplifiers to operate orthogonally at the same time in the same sample. Robust performance is achieved when imaging five target mRNAs simultaneously in fixed whole-mount and sectioned zebrafish embryos. HCR amplifiers exhibit deep sample penetration, high signal-to-background ratios and sharp signal localization.

Each cell in a multicellular organism contains the same genome, yet the regulatory circuits encoded within this genome implement a developmental program yielding significant spatial heterogeneity and complexity. *In situ* hybridization methods are an essential tool for elucidating developmental and pathological processes, enabling imaging of mRNA expression in a morphological context from subcellular to organismal-length scales[1,2,8–21].

Due to variability between biological specimens, the accurate mapping of spatial relationships between regulatory loci of different genes requires multiplexed experiments in which multiple mRNAs are imaged in a single biological sample. Within intact vertebrate embryos, enzymatic *in situ* amplification methods based on catalytic deposition of reporter molecules are currently the method of choice to achieve high signal-to-background ratios[4,5,22,23]. The key difficulty is the lack of orthogonal deposition chemistries, necessitating serial multiplexing approaches in which two[3,5] or three[4,6] target mRNAs are detected in succession using cumbersome procedures that progressively degrade the sample as the number of target mRNAs increases. Here, we overcome this difficulty by programming orthogonal HCR amplifiers[7] that function as independent molecular instruments,

simultaneously reading out the expression patterns of five target mRNAs from within a single intact biological sample.

An HCR amplifier consists of two nucleic acid hairpin species (H1 and H2 in **Fig. 1a**) that are designed to co-exist metastably in the absence of a nucleic acid initiator (I)[7]. Each HCR hairpin consists of an input domain with an exposed single-stranded toehold and an output domain with a single-stranded toehold sequestered in the hairpin loop. Hybridization of the initiator to the input domain of H1 (**Fig. 1a**, '1-2') opens the hairpin to expose its output domain (**Fig. 1a**, '3*-2*'). Hybridization of this output domain to the input domain of H2 (**Fig. 1a**, '2-3') opens the hairpin to expose an output domain (**Fig. 1a**, '2*-1*') identical in sequence to the initiator. Regeneration of the initiator sequence provides the basis for a chain reaction of alternating H1 and H2 polymerization steps leading to formation of a nicked double-stranded 'polymer'. If the initiator is absent, the hairpins are metastable (that is, kinetically impeded from polymerizing) due to the sequestration of the output toeholds in the hairpin loops.
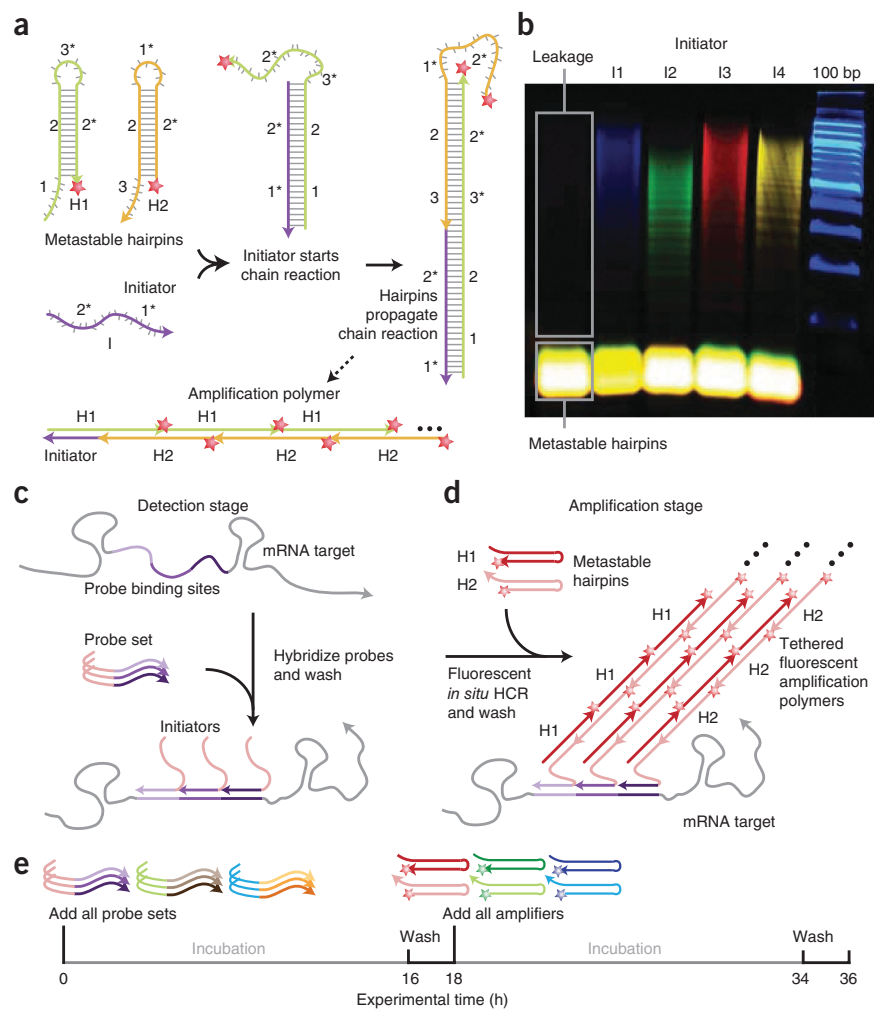
This mechanism has two properties that are important when attempting to achieve simultaneous multiplexed *in situ* amplification in vertebrate embryos. First, the programmable chemistry of nucleic acid base pairing suggests the feasibility of engineering orthogonal HCR amplifiers that operate independently in the same sample at the same time. Second, in contrast to molecular self-assembly by means of traditional annealing protocols in which components interact as soon as they are mixed together[24], HCR is an isothermal triggered self-assembly process. Hence, hairpins should penetrate the sample before undergoing triggered self-assembly *in situ*, suggesting the potential for deep sample penetration and high signal-to-background ratios.

Despite previous successes in implementing HCR in a test tube[7,25], it proved challenging to engineer HCR hairpins for *in situ* hybridization due to the stringent hybridization conditions that are required to destabilize nonspecific binding (40% hybridization buffer; **Supplementary Notes**). The free energy of each HCR polymerization step arises from the enthalpic benefit of forming additional stacked base pairs between the toehold in the output domain at the growing end of the polymer and the toehold in the input domain of a newly recruited hairpin, as well as from the entropic benefit of opening the hairpin loop of the recruited hairpin. The original HCR system used DNA hairpins with 6-nt toeholds and loops and 18-bp stems[7] (resulting in six stacked base pairs plus the opening of a 6-nt hairpin loop per polymerization step). Preliminary test tube and *in situ* hybridization studies revealed

---

[1]Department of Bioengineering, California Institute of Technology, Pasadena, California, USA. [2]Department of Biology, California Institute of Technology, Pasadena, California, USA. [3]Department of Applied & Computational Mathematics, California Institute of Technology, Pasadena, California, USA. Correspondence should be addressed to N.A.P. (niles@caltech.edu).

Figure 1 Multiplexed *in situ* hybridization using fluorescent HCR *in situ* amplification. (**a**) HCR mechanism. Metastable fluorescent RNA hairpins self-assemble into fluorescent amplification polymers upon detection of a specific RNA initiator. Initiator I nucleates with hairpin H1 via base pairing to single-stranded toehold '1', mediating a branch migration[30] that opens the hairpin to form complex I·H1 containing single-stranded segment '3*-2*'. This complex nucleates with hairpin H2 by means of base pairing to toehold '3', mediating a branch migration that opens the hairpin to form complex I·H1·H2 containing single-stranded segment '2*-1*'. Thus, the initiator sequence is regenerated, providing the basis for a chain reaction of alternating H1 and H2 polymerization steps. Red stars denote fluorophores. (**b**) Validation in a test tube. Agarose gel demonstrating orthogonal amplification in a reaction volume containing four HCR amplifiers and zebrafish total RNA. Minimal leakage from metastable states is observed in the absence of initiators. (**c**) Detection stage. Probe sets are hybridized to mRNA targets and then unused probes are washed from the sample. (**d**) Amplification stage. Initiators trigger self-assembly of tethered fluorescent amplification polymers and then unused hairpins are washed from the sample. (**e**) Experimental timeline. The same two-stage protocol is used independent of the number of target mRNAs. For multiplexed experiments (three-color example depicted), probe sets for different target mRNAs carry orthogonal initiators that trigger orthogonal HCR amplification cascades labeled by spectrally distinct fluorophores.

that this small-loop DNA-HCR system did not polymerize under stringent hybridization conditions due to insufficient free energy per polymerization step[26].
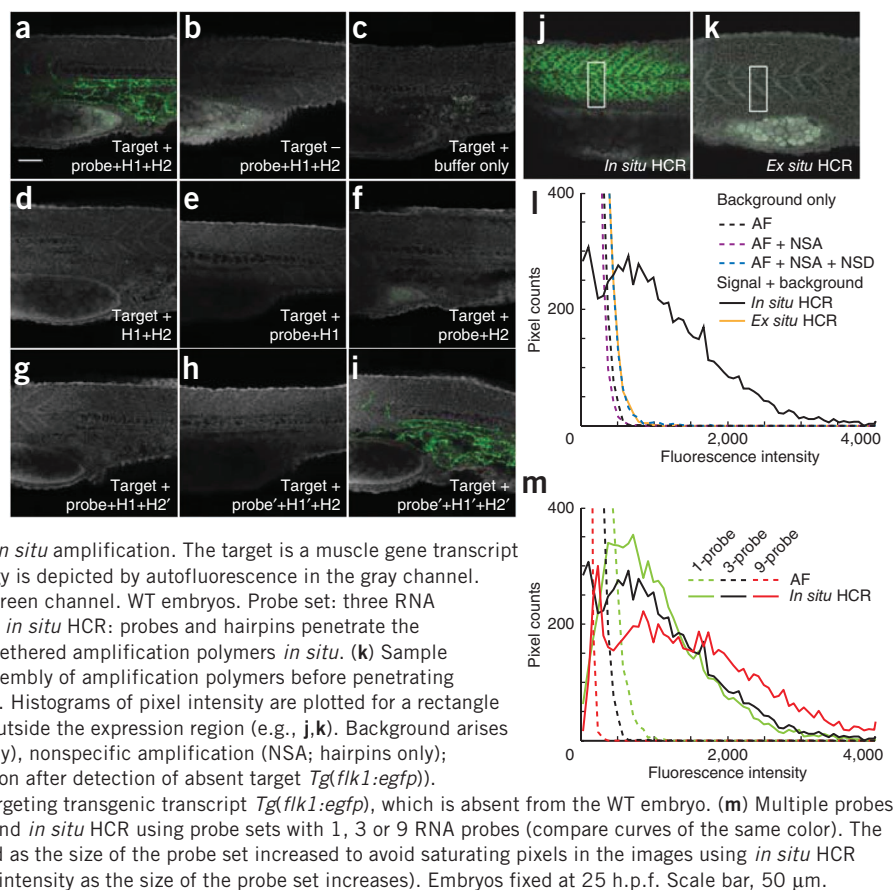
Thus, we confronted the challenge of engineering new HCR hairpins that retain two key properties under these conditions: (i) hairpin metastability in the absence of the initiator, (ii) hairpin polymerization in the presence of the initiator. Previous experience suggested that these two objectives are at odds. Hairpin metastability is promoted by reducing toehold and loop size; hairpin polymerization is promoted by increasing toehold and loop size.

Secondary structure free energy parameters have not been measured for stringent hybridization conditions, so we could not resize components based on computational simulation. Instead, we used test tube and *in situ* control experiments to measure the minimum hairpin toehold and loop length necessary for stable hybridization. Imposing this design constraint to promote hairpin polymerization did not prevent us from retaining hairpin metastability under the same stringent hybridization conditions. To partially counteract the necessary increase in hairpin size, we switched from DNA to RNA hairpins to exploit the enhanced stability of stacked RNA base pairs relative to DNA base pairs. The resulting big-loop RNA-HCR system has 10-nt toeholds and loops and 16-bp stems. The results of the test tube study presented in **Figure 1b** illustrate four HCR amplifiers operating simultaneously and orthogonally in a background of zebrafish total RNA under stringent hybridization conditions. The hairpins exhibit metastability in the absence of initiators; the introduction of a single initiator species selectively triggers the cognate polymerization reaction.

We perform *in situ* hybridization in two stages independent of the number of target mRNAs (**Fig. 1c**–**e**). In the detection stage, all target mRNAs are detected simultaneously via *in situ* hybridization of complementary RNA probes; unused probes are washed from the sample. Each target mRNA is addressed by a probe set comprising one or more RNA probe species carrying identical initiators; different targets are addressed by probe sets carrying orthogonal initiators. In the amplification stage, optical readouts are generated for all target mRNAs simultaneously using fluorescent *in situ* HCR. Orthogonal initiators trigger orthogonal hybridization chain reactions in which metastable RNA hairpins self-assemble into tethered amplification polymers labeled with spectrally distinct fluorophores; unused hairpins are washed from the sample before imaging.

To validate HCR *in situ* amplification in fixed whole-mount zebrafish embryos, we first targeted a transgenic mRNA , observing bright staining with the expected expression pattern (**Fig. 2a**). Wild-type embryos (lacking the target) show minimal staining (**Fig. 2b**), comparable to the autofluorescence observed in the absence of probes and hairpins (**Fig. 2c**). As expected, amplification is not observed if the probe or either of the two hairpin species is omitted (**Fig. 2d**–**f**). To verify that the staining in **Figure 2a** results from the intended polymerization mechanism rather than from aggregation of closed hairpins, alteration of one or both hairpin stem sequences yields the expected loss (**Fig. 2g,h**) and recovery (**Fig. 2i**) of signal.

Figure 2 Validation of fluorescent HCR *in situ* amplification in fixed whole-mount zebrafish embryos. (**a**–**i**) The target is the transgenic transcript *Tg*(*flk1:egfp*), expressed below the notochord and between the somites (see the expression atlas of **Fig. 3a**). Embryo morphology is depicted by autofluorescence in the gray channel. Probe set: 1 RNA probe. Fluorescent staining (green channel) using *in situ* HCR in Target+ (**a**) and Target− (**b**) embryos compared to (green channel) autofluorescence in the absence of probes and hairpins (**c**). No amplification in the absence of probes (**d**) or of one hairpin species (**e**,**f**). Modification of hairpin stem sequences (H1′, H2′) disrupts (**g**,**h**) and restores (**i**) toehold-mediated branch migration, confirming that staining arises from triggered polymerization rather than from random aggregation of hairpins. Typical for zebrafish, the yolk sack (bottom left of each panel) often exhibits autofluorescence. (**j**–**m**) Characterizing

the signal-to-background ratio for fluorescent HCR *in situ* amplification. The target is a muscle gene transcript (*desm*) expressed in the somites. Embryo morphology is depicted by autofluorescence in the gray channel. Pixel intensity histograms are calculated using the green channel. WT embryos. Probe set: three RNA probes, except panel **m**. (**j**) Sample penetration with *in situ* HCR: probes and hairpins penetrate the sample before executing triggered self-assembly of tethered amplification polymers *in situ*. (**k**) Sample penetration with *ex situ* HCR: probes trigger self-assembly of amplification polymers before penetrating the sample. (**l**) Background and signal contributions. Histograms of pixel intensity are plotted for a rectangle partially within the expression region and partially outside the expression region (e.g., **j**,**k**). Background arises from three sources: autofluorescence (AF; buffer only), nonspecific amplification (NSA; hairpins only); nonspecific detection (NSD; *in situ* HCR amplification after detection of absent target *Tg*(*flk1:egfp*)). NSD studies use a probe set of three RNA probes targeting transgenic transcript *Tg*(*flk1:egfp*), which is absent from the WT embryo. (**m**) Multiple probes per mRNA target. Comparison of autofluorescence and *in situ* HCR using probe sets with 1, 3 or 9 RNA probes (compare curves of the same color). The microscope photomultiplier tube gain was decreased as the size of the probe set increased to avoid saturating pixels in the images using *in situ* HCR amplification (this accounts for the reduction in AF intensity as the size of the probe set increases). Embryos fixed at 25 h.p.f. Scale bar, 50 μm.

Detection and amplification components must successfully penetrate an embryo to generate signal at the site of an mRNA target. HCR is a triggered self-assembly mechanism, offering the conceptual benefit that small RNA probes and hairpins penetrate the embryo before generating larger, less-mobile amplification polymers at the site of mRNA targets. To assess the practical significance of these properties, we imaged an endogenous mRNA with a superficial expression pattern, comparing *in situ* HCR to the *ex situ* HCR alternative in which amplification polymers are pre-assembled before penetrating the sample. The images of **Figure 2j**,**k** and the pixel-intensity histograms of **Figure 2l** demonstrate dramatic signal loss using *ex situ* HCR. This result is consistent with the general experience that large, multilabeled probes suffer from reduced sample penetration and confirms that it is desirable to penetrate the sample with small components that self-assemble in a triggered fashion at the site of mRNA targets.

In situ amplification is intended to generate a high signal-to-background ratio to enable accurate mapping of mRNA expression patterns. With our approach, signal is produced when specifically hybridized probes initiate specific HCR amplification to yield fluorescent polymers tethered to cognate mRNA targets. Background can arise from three sources: nonspecific detection (probes that bind nonspecifically and are subsequently amplified), nonspecific amplification (hairpins and polymers that are not hybridized to cognate initiators) and autofluorescence (inherent fluorescence of the fixed embryo). To characterize the relative magnitudes of these effects, we imaged an mRNA target with a sharply defined region of expression and plotted histograms of pixel intensity within a rectangle that crosses the boundary of this expression region. The pixel intensity histograms of **Figure 2l** reveal that autofluorescence is the primary source of background, that nonspecific
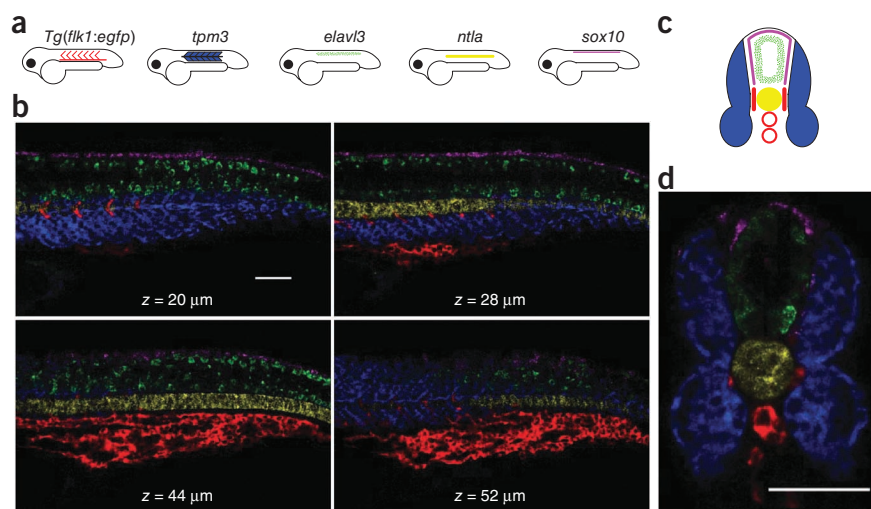
detection contributes a small amount of additional background and that nonspecific amplification contributes negligibly to background. By comparison, the signal generated using *in situ* HCR amplification yields pixel intensities that are significantly higher than background.

The observation that autofluorescence is the dominant source of background suggests that addressing each target mRNA with a probe set comprising multiple probes[13,19] would further increase the signal-to-background ratio. Subsequent HCR *in situ* amplification would then decorate each target with an array of amplification polymers. **Figure 2m** demonstrates that the ratio of signal to autofluorescence increases with the number of probes per target. Notably, using *in situ* HCR, the pixel intensity distribution is bimodal using either three or nine probes per target, with a peak at low intensity corresponding to background (from the portion of the rectangle outside the expression region) and a broad distribution at higher intensities corresponding to signal (from the portion of the rectangle within the expression region). High signal-to-background is demonstrated for a target mRNA with a lower level of expression in **Supplementary Notes**.

The fundamental benefit of using orthogonal HCR amplifiers is the ability to perform simultaneous *in situ* amplification for multiple target mRNAs, enabling straightforward multiplexing. **Figure 3** demonstrates simultaneous imaging of five target mRNAs in fixed whole-mount and cross-sectioned zebrafish embryos. Targets were detected using five probe sets carrying five orthogonal initiators and amplification was performed using five orthogonal HCR amplifiers carrying five spectrally distinct fluorophores. The expression patterns in the cross-sectioned embryo confirm that HCR signal survives vibratome sectioning.

Using HCR *in situ* amplification, each amplification polymer is expected to remain tethered to its initiating probe, suggesting the

Figure 3 Multiplexed imaging in fixed whole-mount and cross-sectioned zebrafish embryos. (**a**) Expression atlas for five target mRNAs (lateral view: *Tg(flk1:egfp)*, *tpm3*, *elavl3*, *ntla*, *sox10*). (**b**) mRNA expression imaged using confocal microscopy at four planes within an embryo. This multiplexed experiment is performed using the same two-stage protocol that is used for single-color experiments (summarized in **Fig. 1c–e**). Detection is performed using five probe sets carrying orthogonal initiators. The probe sets have different numbers of RNA probes (10,7,18,30,20) based on the strength of expression of each mRNA target and the strength of the autofluorescence in each channel. Amplification is performed using five orthogonal HCR amplifiers carrying spectrally distinct fluorophores. (**c**) Expression atlas for five target mRNAs (anterior view). (**d**) mRNA expression imaged within a 200-μm zebrafish section using confocal microscopy. Vibratome sectioning was performed after HCR *in situ* amplification and post-fixation. See also the image stacks of **Supplementary Movies 1** and **2**. Embryos fixed at 27 h.p.f. Scale bars, 50 μm.

potential for accurate signal localization and co-localization. Here, we test signal localization and co-localization using a four-color, two-target experiment in which one target mRNA is expressed predominantly in the somites and the other is expressed predominantly in the interstices of somites. The two target mRNAs are each detected using two independent probe sets and each of the four probe sets is amplified using a spectrally distinct HCR amplifier. Double detection of a single target mRNA provides a rigorous test of signal co-localization independent of the expression pattern of the target. **Figure 4a,b** reveals sharp co-localization of two signals for each of the two target mRNAs.

Simultaneous mapping of two targets expressed in contiguous cells provides a further test of signal localization. **Figure 4c** demonstrates interleaving of two sharp expression patterns, revealing that the interstitial expression pattern between somites is only the width of a single stretched cell. This study suggests that HCR polymers remain tethered to their initiating probes and demonstrates sharp signal localization and co-localization at the level of single cells within whole-mount zebrafish embryos.

The sequencing of numerous genomes has launched a new era in biology, enabling powerful comparative approaches and revealing the nucleotide sequences that contribute to the differences between species, between individuals of the same species and between cells within an individual. However, knowledge of these sequences is not sufficient to reveal the architecture and function of the biological circuits that account for these differences. Much work remains to
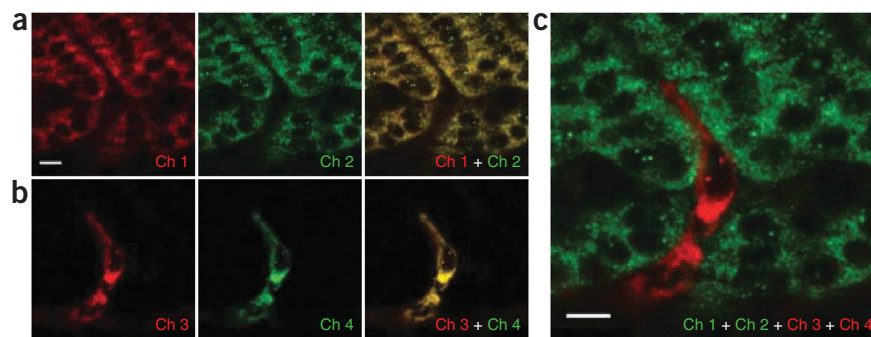
elucidate both the details and the principles of the molecular circuits that regulate development, maintenance, repair and disease within living organisms.

Over four decades[8], *in situ* hybridization methods have become an indispensible tool for the study of genetic regulation in a morphological context. Current methods of choice for performing enzymatic *in situ* amplification in vertebrate embryos require serial amplification for multiplexed studies[3–6,22,23]. This shortcoming is a major impediment to the study of interacting regulatory elements *in situ*. For example, simultaneous mapping of three target mRNAs in whole-mount chick embryos requires 5 d using serial *in situ* amplification approaches[4,6].

In recent years, researchers in the field of nucleic acid nanotechnology have made much progress in designing nucleic acid molecules that interact and change conformation to execute diverse dynamic functions[27–29]. Here, we exploit design principles drawn from this experience to engineer small conditional RNAs that interact and change conformation to amplify the expression patterns of multiple target mRNAs in parallel within intact vertebrate embryos. The resulting programmable molecular technology addresses a longstanding need in the biological sciences.

HCR *in situ* amplification enables simultaneous mapping of five target mRNAs in fixed whole-mount and sectioned zebrafish embryos. The programmability and sequence specificity of the HCR mechanism enable all five amplifiers to operate orthogonally in the same sample at the same time. Hence, the time required to map five targets is the

Figure 4 Sharp signal localization and co-localization in fixed whole-mount zebrafish embryos. Redundant two-color mapping of one target mRNA expressed predominantly in the somites (*desm*; two probe sets, two HCR amplifiers, channels 1 and 2) simultaneous with redundant two-color mapping of a second target mRNA expressed predominantly in the interstices of somites (*Tg(flk1:egfp)*: two probe sets, two HCR amplifiers, channels 3 and 4). (**a**) Sharp co-localization of *desm* signal (Pearson correlation coefficient, $r = 0.93$). (**b**) Sharp co-localization of *Tg(flk1: egfp)* signal (Pearson correlation coefficient, $r = 0.97$). (**c**) Sharp signal localization within the two interleaved expression regions. The interstice between somites is only the width of a single stretched cell. Embryos fixed at 27 h.p.f. Scale bars, 10 μm.

same as that required to map one target and the sample degradation that accompanies sequential detection of multiple mRNAs is avoided. We observe that autofluorescence, rather than nonspecific detection or nonspecific amplification, is the dominant source of background in zebrafish. Consequently, the signal-to-background ratio is enhanced by using probe sets with multiple probes, each carrying an HCR initiator. Small fluorophore-labeled amplification components penetrate the sample before undergoing triggered self-assembly to form fluorescent amplification polymers that remain tethered to their initiating probes. The triggered self-assembly property leads to a high signal-to-background ratio and deep sample penetration. The tethering property leads to sharp signal localization and co-localization at the level of single cells within whole-mount zebrafish embryos.

Our approach is potentially suited for use in a variety of biological contexts including fixed cells, embryos, tissue sections and microbial populations. By coupling HCR initiators to aptamer or antibody probes, HCR amplification is also potentially suitable for extension to multiplexed imaging of small molecules and proteins. Further work is required to explore these possibilities.

The HCR amplifiers presented here are suitable for use with diverse mRNA targets because the initiator sequences (and consequently the HCR hairpins) are independent of the mRNA target sequences. Imaging a new target mRNA requires only a new probe set with each probe carrying an HCR initiator.

METHODS

Methods and any associated references are available in the online version of the paper at http://www.nature.com/naturebiotechnology/.

Note: Supplementary information is available on the Nature Biotechnology website.

1. Qian, X., Jin, L. & Lloyd, R.V. In situ hybridization: basic approaches and recent development. *J. Histotechnol.* **27**, 53–67 (2004).
2. Silverman, A. & Kool, E. Oligonucleotide probes for RNA-targeted fluorescence in situ hybridization. *Adv. Clin. Chem.* **43**, 79–115 (2007).
3. Thisse, B. *et al.* Spatial and temporal expression of the zebrafish genome by large-scale in situ hybridization screening. in *Zebrafish: Genetics, Genomics and Informatics*, vol. 77, edn. 2 (eds. Detrich, H.W., Zon, L.I. & Westerfield, M.) 505–519 (Elsevier, 2004).
4. Denkers, N., Garcia-Villalba, P., Rodesch, C.K., Nielson, K.R. & Mauch, T.J. FISHing for chick genes: Triple-label whole-mount fluorescence in situ hybridization detects simultaneous and overlapping gene expression in avian embryos. *Dev. Dyn.* **229**, 651–657 (2004).
5. Barroso-Chinea, P. *et al.* Detection of two different mRNAs in a single section by dual in situ hybridization: A comparison between colorimetric and fluorescent detection. *J. Neurosci. Methods* **162**, 119–128 (2007).
6. Acloque, H., Wilkinson, D.G. & Nieto, M.A. In situ hybridization analysis of chick embryos in whole-mount and tissue sections. in *Avian Embryology, 2nd Edition* vol. 87 (ed. Bronner-Fraser, M.) 169–185 (Elsevier, 2008).
7. Dirks, R.M. & Pierce, N.A. Triggered amplification by hybridization chain reaction. *Proc. Natl. Acad. Sci. USA* **101**, 15275–15278 (2004).
8. Gall, J.G. & Pardue, M.L. Formation and detection of RNA-DNA hybrid molecules in cytological preparations. *Proc. Natl. Acad. Sci. USA* **63**, 378–383 (1969).
9. Lawrence, J.B., Singer, R.H. & Marselle, L.M. Highly localized tracks of specific transcripts within interphase nuclei visualized by in situ hybridization. *Cell* **57**, 493–502 (1989).
10. Tautz, D. & Pfeifle, C. A non-radioactive in situ hybridization method for the localization of specific RNAs in *Drosophila* embryos reveals translational control of the segmentation gene hunchback. *Chromosoma* **98**, 81–85 (1989).
11. Kislauskis, E.H., Li, Z., Singer, R.H. & Taneja, K.L. Isoform-specific 3′-untranslated sequences sort α-cardiac and β-cytoplasmic actin messenger RNAs to different cytoplasmic compartments. *J. Cell. Biol.* **123**, 165–172 (1993).
12. O'Neill, J.W. & Bier, E. Double-label in situ hybridization using biotin digoxigenin-tagged RNA probes. *Biotechniques* **17**, 870–875 (1994).
13. Femino, A.M., Fay, F.S., Fogarty, K. & Singer, R.H. Visualization of single RNA transcripts in situ. *Science* **280**, 585–590 (1998).
14. Zaidi, A.U., Enomoto, H., Milbrandt, J. & Roth, K.A. Dual fluorescent in situ hybridization and immunohistochemical detection with tyramide signal amplification. *J. Histochem. Cytochem.* **48**, 1369–1375 (2000).
15. Player, A.N., Shen, L.-P., Kenny, D., Antao, V.P. & Kolberg, J.A. Single-copy gene detection using branched DNA (bDNA) in situ hybridization. *J. Histochem. Cytochem.* **49**, 603–612 (2001).
16. Levsky, J.M., Shenoy, S.M., Pezo, R.C. & Singer, R.H. Single-cell gene expression profiling. *Science* **297**, 836–840 (2002).
17. Kosman, D. *et al.* Multiplex detection of RNA expression in *Drosophila* embryos. *Science* **305**, 846 (2004).
18. Lambros, M.B.K., Natrajan, R. & Reis-Filho, J.S. Chromogenic and fluorescent in situ hybridization in breast cancer. *Hum. Pathol.* **38**, 1105–1122 (2007).
19. Raj, A., van den Bogaard, P., Rifkin, S.A., van Oudenaarden, A. & Tyagi, S. Imaging individual mRNA molecules using multiple singly labeled probes. *Nat. Methods* **5**, 877–879 (2008).
20. Amann, R. & Fuchs, B.M. Single-cell identification in microbial communities by improved fluorescence in situ hybridization techniques. *Nat. Rev. Microbiol.* **6**, 339–348 (2008).
21. Larsson, C., Grundberg, I., Soderberg, O. & Nilsson, M. *In situ* detection and genotyping of individual mRNA molecules. *Nat. Methods* **7**, 395–397 (2010).
22. Harland, R.M. In situ hybridization: an improved whole-mount method for *Xenopus* embryos. *Methods Cell Biol.* **36**, 685–695 (1991).
23. Speel, E.J.M., Hopman, A.H.N. & Komminoth, P. Amplification methods to increase the sensitivity of in situ hybridization: Play CARD(S). *J. Histochem. Cytochem.* **47**, 281–288 (1999).
24. Feldkamp, U. & Niemeyer, C.M. Rational design of DNA nanoarchitectures. *Angew Chem. Int. Ed.* **45**, 1856–1876 (2006).
25. Venkataraman, S., Dirks, R.M., Rothemund, P.W.K., Winfree, E. & Pierce, N.A. An autonomous polymerization motor powered by DNA hybridization. *Nat. Nanotechnol.* **2**, 490–494 (2007).
26. Choi, H.M.T. *Programmable In Situ Amplification for Multiplexed Bioimaging.* PhD thesis, California Institute of Technology (2009).
27. Simmel, F.C. & Dittmer, W.U. DNA nanodevices. *Small* **1**, 284–299 (2005).
28. Bath, J. & Turberfield, A.J. DNA nanomachines. *Nat. Nanotechnol.* **2**, 275–284 (2007).
29. Feldkamp, U. & Niemeyer, C.M. Rational engineering of dynamic DNA systems. *Angew. Chem. Int. Ed.* **47**, 3871–3873 (2008).
30. Yurke, B., Turberfield, A.J., Mills, J.A.P., Simmel, F.C. & Neumann, J.L. A DNA-fuelled molecular machine made of DNA. *Nature* **406**, 605–608 (2000).

ONLINE METHODS

Probe synthesis. RNA probes are 81-nt long (26-nt initiator, 5-nt spacer, 50-nt mRNA recognition sequence). mRNAs are addressed by probe sets containing one or more probes that hybridize adjacently at 50-nt binding sites. Probe sequences are displayed in **Supplementary Notes**. RNA probes were synthesized by *in vitro* transcription. The coding strand for each probe contained three random nucleotides and a 19-nt SP6 promoter sequence upstream of the 81-nt initiator-linker-probe sequence. Complementary DNA coding and template strands were ordered (unpurified) from Integrated DNA Technologies (IDT). Strands were resuspended in ultrapure water (resistance of 18 MΩ cm) and concentrations were determined by measuring absorption at 260 nm. The double-stranded template was formed by annealing the two strands (heat at 95 °C for 5 min, cool 1 °C/min to 25 °C) in $1 \times$ SPSC buffer (0.4 M NaCl, 50 mM Na_2HPO_4, pH 7.5). RNA probes were transcribed overnight at 37 °C using an AmpliScribe SP6 high yield transcription kit (Epicentre Biotechnologies) with four unmodified ribonucleotide triphosphates. Probes were purified using an RNeasy mini kit (Qiagen) and concentrations were determined by measuring absorbance at 260 nm.

HCR hairpin design. RNA HCR hairpins are 52-nt long (10-nt toehold, 16-bp stem, 10-nt loop). Hairpin sizing was based on *in vitro* and *in situ* binding studies performed in 40% hybridization buffer[26]. HCR hairpin sequences were designed by considering a set of target secondary structures involving different subsets of the strands (I, H1, H2, I·H1 and I·H1·H2, each as depicted in **Fig. 1a**). For a given target secondary structure, the ensemble defect represents the average number of incorrectly paired nucleotides at equilibrium, calculated over the ensemble of unpseudoknotted secondary structures[31,32]. Sequence design was performed by mutating the hairpin sequences so as to reduce the sum of the calculated ensemble defects over the set of target structures (J.N. Zadeh, personal communication). Multiple HCR amplifiers were designed independently and then sequence orthogonality was checked using NUPACK (http://www.nupack.org/)[33] to simulate the equilibrium species concentrations and base pairing properties for a test tube[34] containing different subsets of strands. This approach was used to check for off-target interactions between each of the five initiators and the other four hairpin sets, as well as between the 10-nt toehold and loop segments of each hairpin set and the 10-nt toehold and loop segments of the other four hairpin sets. The sequences are shown in **Supplementary Notes**.

HCR hairpin synthesis. Each HCR hairpin was synthesized by IDT as two segments with one segment end-labeled with an amine (3′-end for H1 and 5′-end for H2) to permit subsequent coupling to a fluorophore. The strand with a 5′ end at the ligation site was ordered with a 5′ phosphate to permit ligation. Ligation of the two segments produced the full 52-nt hairpin. The ligation was performed using T4 RNA ligase 2 (New England Biolabs) at 16 °C for a minimum of 8 h. The ligated strands were purified using a 15% denaturing polyacrylamide gel. The bands corresponding to the expected sizes of the ligated products were visualized by UV shadowing and excised from the gel. The RNA strands were then eluted by soaking in 0.3 M NaCl overnight and recovered by ethanol precipitation. The pellet was dried and resuspended in ultrapure water and quantified by measuring absorbance at 260 nm. The dye coupling reaction was performed by mixing an amine-labeled hairpin with an Alexa Fluor succinimidyl ester (Invitrogen) and incubating in the dark for 3 h. Alexa-labeled hairpins were separated from unincorporated dyes by repeating the denaturing PAGE purification described above. To ensure that H1 and H2 form hairpin monomers, the strands were snap-cooled in $1 \times$ SPSC buffer before use (heat at 95 °C for 90 s, cool to room temperature (~23 °C) on the benchtop for 30 min).

Multiplexed gel electrophoresis. Reactions for **Figure 1b** were performed in 40% hybridization buffer (HB) without blocking agents (40% formamide, $2 \times$ SSC, 9 mM citric acid (pH 6.0), 0.1% Tween 20) with 0.1 µg/µl of total RNA extracted from zebrafish using TRIzol (Invitrogen). Each of the eight hairpin species (two for each of the four HCR amplifiers) was snap-cooled at 3 µM in $1 \times$ SPSC buffer. The RNA initiator for each HCR system was diluted to 0.3 µM in ultrapure water. Each lane was prepared by mixing 12 µl of formamide, 6 µl of $5 \times$ HB supplements without blocking agents ($10 \times$ SSC, 45 mM citric acid (pH 6.0),

0.5% Tween 20), 1.76 µl of 1.7 µg/µl extracted zebrafish total RNA and 1 µl of each of the eight hairpins. When an initiator was absent (lane 1), 2.24 µl of ultrapure water was added to bring the reaction volume to 30 µl. For lanes 2 to 5, 1 µl of 0.3 µM initiator for one HCR amplifier and 1.24 µl of ultrapure water were added. The reactions were incubated at 45 °C for 1.5 h. The samples were supplemented with 7.5 µl of 50% glycerol and loaded into a native 2% agarose gel, prepared with $1 \times$ lithium boric acid buffer (LB) (Faster Better Media). The gel was run at 150 V for 90 min at room temperature and imaged using an FLA-5100 fluorescent scanner (Fujifilm Life Science). The excitation laser sources and emission filters were as follows: a 473 nm laser and a 530 ± 10 nm bandpass filter (amplifier HCR3, Alexa 488), a 532 nm laser and a 570 ± 10 nm bandpass filter (amplifier HCR5, Alexa 546), a 635 nm laser and a 665 longpass filter (amplifier HCR1, Alexa 647) and a 670 nm laser and a 705 nm longpass filter (amplifier HCR4, Alexa 700).

***In situ* hybridization studies.** Procedures for the care and use of zebrafish embryos were approved by the Caltech IACUC. Embryos were fixed and permeablized using the protocol described in **Supplementary Notes**. For the transgenic samples, GFP+ embryos were identified using a Leica MZ16 FA fluorescence stereomicroscope. *In situ* hybridization experiments for **Figures 2–4** were performed using the protocol provided in **Supplementary Notes**. Overnight incubations were performed for 16 h. For **Figure 2a–i**, probe solution was prepared by introducing 6 pmol of each probe (1–3 µl depending on the stock solution) into 300 µl of 50% HB at 55 °C. Hairpin solution was prepared by introducing 10 pmol of each hairpin (snap-cooled in 5 µl) into 300 µl of 40% HB at 45 °C. For **Figure 2j–m**, experiments were performed using WT embryos. A probe set with three probes (1 pmol of each probe) was used for **Figure 2j–l**; probe sets with 1, 3 or 9 probes (1 pmol of each probe) were used for **Figure 2m**. The standard *in situ* protocol was used for both the (AF + NSA) sample (with probes excluded) and for the AF sample (with probes and hairpins excluded). For the (AF + NSA + NSD) sample, *desm* probes were replaced with *egfp* probes carrying the same initiator sequence as the *desm* probes. For the *ex situ* HCR study of **Figure 2k,l**, snap-cooled hairpins (30 pmol of each hairpin) and probes (1 pmol of each probe) were added to 300 µl of 40% HB and incubated at 45 °C for 16 h while the embryos were incubated without probes in 50% HB at 55 °C. For consistency, these embryos were subjected to the standard probe washes and the standard amplification protocol (substituting the pre-assembled polymer solution for the hairpin solution). Experiments for **Figures 3** and **4** were performed with *Tg(flk1:egfp)* embryos using probe and hairpin solutions prepared following the protocol in **Supplementary Notes**.

Vibratome sectioning. After completion of the standard *in situ* protocol (**Supplementary Notes**), embryos were post-fixed with 4% paraformaldehyde at room temperature for 20 min. Fixation was stopped by washing the embryos three times with $1 \times$ PBST. Embryos were then embedded in 4% low-melting agarose (Cambrex) in $1 \times$ PBST and sectioned into 200 µm slices with a Vibratome Series 1000 tissue sectioning system (Vibratome).

Confocal microscopy. A chamber for mounting the embryo was made by aligning 2 stacks of Scotch tape (eight pieces per stack) 1 cm apart on a 25 mm × 75 mm glass slide (VWR). Approximately 200 µl of 3% methyl cellulose mounting medium was added between the tape stacks on the slide and embryos were placed on the medium oriented for lateral imaging. A 22 mm × 22 mm no. 1 coverslip (VWR) was placed on top of the stacks to close the chamber. The sectioned sample of **Figure 3d** was mounted using a SlowFade Gold antifade reagent (Molecular Probes). A Zeiss 510 upright confocal microscope with an LD LCI Plan-Apochromat 25×/0.8 Imm Corr DIC objective was used to acquire the images for **Figure 2**. The excitation laser sources and emissions filters were: 488 nm Ar laser excitation source and a 520 ± 10 nm bandpass filter (gray; autofluorescence), 633 nm HeNe laser and a 650 nm long pass filter (green; Alexa 647). A Leica TCS SP5 inverted confocal microscope with an HCX PL APO 20×/0.7 Imm objective was used to acquire the five-color images of **Figure 3b,d**. Excitation laser sources and emissions bandpass filters were as follows: 488 nm/500–540 nm (Alexa 488), 514 nm/550–565 nm (Alexa 514), 543 nm/550–605 nm (Alexa 546), 594 nm/605–640 nm (Alexa 594), 633 nm/655–720 nm (Alexa 647). Cluster analysis (Leica) was performed

to enhance dye separation. A Zeiss 510 META NLO inverted confocal microscope with an LD C-Apochromat 40×/1.1 W Corr objective was used to acquire the images for **Figure 4**. Excitation laser sources and emission filters were: 488 nm/tunable 500–522 nm (Alexa 488), 514 nm/tunable 543–586 nm (Alexa514), 561 nm/575–630 nm (Alexa 594), 633 nm/650–710 nm (Alexa 647). For the images of **Figure 4**, image registration (rigid body translation and rotation) was performed to correct for possible misalignment between the two channels (TurboReg plugin for ImageJ). All images are presented without background subtraction.

31. Dirks, R.M., Lin, M., Winfree, E. & Pierce, N.A. Paradigms for computational nucleic acid design. *Nucleic Acids Res.* **32**, 1392–1403 (2004).
32. Zadeh, J.N., Wolfe, B.R. & Pierce, N.A. Nucleic acid sequence design via efficient ensemble defect optimization. *J. Compu. Chem.* published online, doi:10.1002/jcc.2163 (17 August 2010).
33. Zadeh, J.N. *et al.* NUPACK: analysis and design of nucleic acid systems. *J. Compu. Chem.* published online, doi:10.1002/jcc.21596 (19 July 2010).
34. Dirks, R.M., Bois, J.S., Schaeffer, J.M., Winfree, E. & Pierce, N.A. Thermodynamic analysis of interacting nucleic acid strands. *SIAM Rev.* **49**, 65–88 (2007).